Journal of Geodynamics 48 (2009) 284–291

Contents lists available at ScienceDirect

Journal of Geodynamics

journal homepage: http://www.elsevier.com/locate/jog

Expected temporal absolute gravity change across the Taiwanese Orogen, a modeling approach

M. Mouyen[a,*], F. Masson[a], C. Hwang[b], C.-C. Cheng[b], R. Cattin[c], C.W. Lee[d], N. Le Moigne[c], J. Hinderer[a], J. Malavieille[c], R. Bayer[c], B. Luck[a]

[a] Institut de Physique du Globe de Strasbourg, 5 rue René Descartes, F-67084 Strasbourg Cedex, France
[b] Department of Civil Engineering, National Chiao Tung University, 1001 University Road, Hsinchu, 300 Taiwan, ROC
[c] Géosciences Montpellier, Université Montpellier 2, Place E. Bataillon, 34095 Montpellier Cedex 5, France
[d] Center for Measurement Standards, Industrial Technology Research Institute, 195 Chung Hsing Rd., Sec.4 Chu Tung, HsinChu, 310 Taiwan, ROC

ARTICLE INFO

Keywords:
Taiwan
Gravity
Modeling
Surrection
Mass transfers

ABSTRACT

The island of Taiwan is located on the convergent boundary between the Philippine Sea plate and the Chinese continental margin. It offers very active mountain building and collapsing processes well illustrated by the rugged topography, rapid uplift and denudation, young tectonic landforms, active faulting and numerous earthquakes. In this paper, using simple models, we have estimated vertical movements and associated absolute gravity variations which can be expected along a profile crossing the southern part of the island and probably suffering the highest rates of rising. The two different tectonic styles proposed for the island, thin-skinned and thick-skinned, were taken into account. Horizontal and vertical movements were modeled by an elastic deformation code. Gravity variations due to these deformations are then modeled at a second step. They are dominated by plate and free-air effects, i.e. elevation of the topography, with several $\mu Gal\,yr^{-1}$. By comparison, gravity changes generated by mass transfers are weak: maximum 0.1 $\mu Gal\,yr^{-1}$ with the thin-skinned tectonic and 0.3 $\mu Gal\,yr^{-1}$ with the thick-skinned tectonic. Though elastic rheology has limitations, this modeling offers interesting results on what gravity signal can be expected from the AGTO project (Absolute Gravity in the Taiwanese Orogen), which proposes to study the dynamic of these mountain ranges using absolute gravimetry (AG) and also including relative gravimetry (RG) and GPS measurements.

1. Introduction

Global positioning system (GPS) and absolute gravimetry are useful tools to study vertical movements and mass transfers involved in mountain building (Segall and Davis, 1997; Torge, 1990). Combining both tools improves understanding of tectonic processes. As an application Karner and Watts (1983) showed how the variation of the ratio between gravity rate and elevation rate across a mountain range can be related to the elastic thickness of the crust.

The AGTO project proposes to study the Taiwan orogeny using absolute and relative gravity measurements, GPS and modeling, in order to jointly identify vertical movements and mass transfer. Taiwan, experiencing vigorous mountain building processes, is a convergence zone located West of south China, between the Chinese Sea and the Philippine Sea (Fig. 1a). The AGTO project is part of two issues. First is to validate the use of absolute gravity for tectonic purposes. Second is to improve our understanding of the Taiwanese orogeny providing information on vertical movements and mass transfers.

The AGTO project focuses on the south part of Taiwan, along a East–West transect crossing the whole island (Fig. 1b). Nine sites have been defined for absolute gravity measurements, close to permanent GPS stations from the Taiwan GPS network. A concrete pillar has been built at each site to put the FG5 absolute gravimeter. In addition a wider network of 53 sites around this transect has been defined for relative gravity measurements (Fig. 1b). It is divided into 9 loops, each containing at least one AG site. This relative gravity network has also been carefully mapped on the Taiwan GPS network, for precise correlation between the gravity signal and the elevation rate. The absolute gravity measurement are repeated every year, using French and Taiwanese FG5 gravimeters. Scintrex CG5 gravimeters are used for the relative network.

The AGTO project is still at its beginning and no conclusion is available yet. In this article, using a modeling approach, we try to characterize gravity variations expected. We start from a 2D structural section of Taiwan and we model the elastic deformation that

* Corresponding author. Tel.: +33 3 90 24 00 77; fax: +33 3 90 24 02 91.
E-mail address: maxime.mouyen@eost.u-strasbg.fr (M. Mouyen).

0264-3707/$ – see front matter © 2009 Elsevier Ltd. All rights reserved.
doi:10.1016/j.jog.2009.09.004

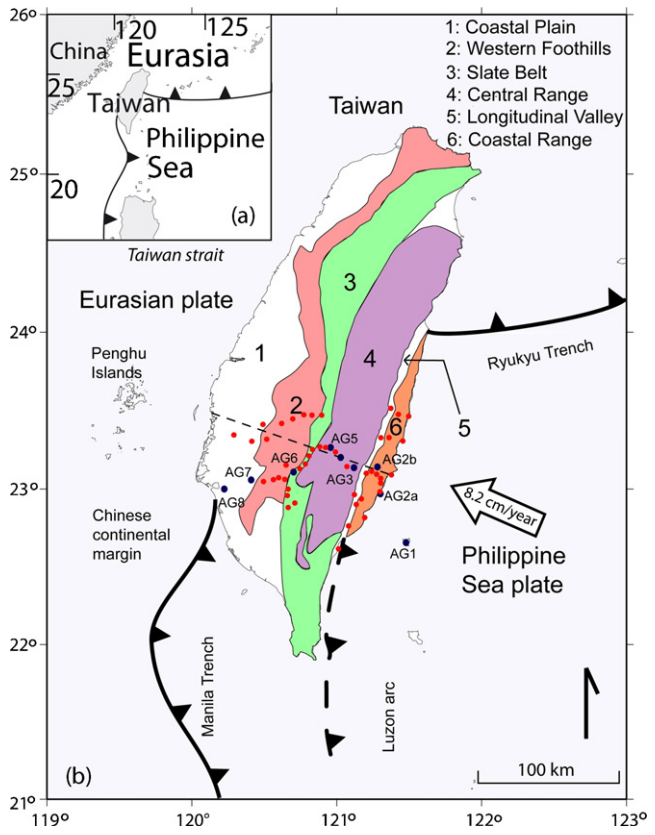

Fig. 1. (a) Global location and plate tectonic settings, (b) general geology of Taiwan after Ho (1986) and Hickman et al. (2002). The nine sites for absolute gravity measurements of the AGTO project, from AG1 to AG8, are represented (blue dots) with also the 45 sites defined for relative gravity measurements network (red dots). Our 2D modeling study is performed along the dashed line. (For interpretation of the references to color in this figure legend, the reader is referred to the web version of the article.)

we constrain with horizontal GPS velocities. Once the modeled horizontal movements fit the measured ones, densities are assigned to Taiwan regions, depending on their geology. Combining deformations and densities, a change in the gravity signal is finally modeled. Two programs have been used to perform this modeling: one for the elastic deformation and one for the gravity change.

After making a global overview of the tectonic context in Taiwan region, we will describe the results we obtained from the elastic modeling and its gravity implication.

2. Tectonic settings

Taiwan island is at the junction of the Philippine Sea plate and the Eurasian plate (Fig. 1a) and results from the convergence of the Luzon volcanic arc on the Philippine Sea plate toward the Chinese continental margin on the Eurasian plate. In the North–East, the Philippine Sea plate is subducted beneath the Eurasian plate. This is expressed by the Ryukyu Trench in the sea ground. More to the South, the situation is the opposite; the Eurasian plate is subducted by the Philippine Sea plate, generating the Manila Trench (Angelier, 1986). In Taiwan, the plate boundary is underlined by the Longitudinal Valley separating the Eurasian plate to the West and the Philippine Sea plate to the East.

The collision between the Luzon arc and the Chinese continental margin started 6.5 Myr. ago in the North of the island. Owing to oblique convergence of these two regions, collision is progressing southward at a rate of 31 mm yr^{-1} (Simoes and Avouac, 2006). Today the Taiwanese orogen reach an altitude of ~4000 m and is still growing (Ho, 1986; Simoes and Avouac, 2006). Ho (1986) divided Taiwan into five geological regions (Fig. 1b). From West to East he identified the Coastal Plain, the Western foothills, the Slate Belt, the Central Range and the Coastal Range. We keep this nomenclature in the following study. The Coastal Plain is made of Neogene sediments overlapped by quaternary alluvium, without relief. The apparition of topography to the East indicates the beginning of the Western Foothills, a fold-and-thrust belt. It extends to the East up to the Tulungwan fault. The Slate Belt is bounded by this fault to the West and by the Lishan fault to the East. It is mostly constituted by Eocene to Oligocene sediments. The Central Range, from the East of Lishan fault to the Longitudinal Valley, is the most deformed part of the Taiwan orogen. It shows Cenozoic clays with moderate metamorphism on its west flank and more metamorphised rocks from the pre-Tertiary basement (Eurasian Continental crust) on its East flank. The Longitudinal Valley is a narrow topographic depression limiting the Central range and the Coastal Range. It contains the Longitudinal Valley fault, the suture zone between the Eurasian end Philippine sea plates. At last, to the eastern part, the Coastal Range, a remnant part of the Luzon volcanic arc mainly constituted by Neogene andesite rocks and turbitite sediments, increases the topography.

Collision, orogeny and subduction processes in Taiwan are among the most vigorous of the Earth and make this region tectonically very active. A first explanation of such activity is the fast convergence of the Philippine Sea plate toward the Eurasian plate, which has been evaluated to 82 mm yr (Yu et al., 1997). High ground movements have been measured by GPS and a high seismicity rate is also recorded due to subduction and numerous active faults. The 1999 Chi–Chi earthquake on the Chelungpu fault, the largest event recorded in Taiwan (Mw = 7.6), illustrates this activity.

No tectonic style of the collision between the Luzon arc and the Chinese continental margin is unanimously accepted. Two main hypothesis are generally discussed: the thin-skinned tectonic (Suppe, 1980; Davis et al., 1983; Dahlen et al., 1984) and the thick-skinned tectonic (Wu et al., 1997; Hung et al., 1999; Mouthereau and Petit, 2003). The geometry of the island cross-sections will be different depending on the hypothesis taken into account and, consequently, the results of the modeling too. As the aim of this study is not to choose between one of these two tectonics but only to see their effects in term of gravity, both will be used.

2.1. Thin-skinned tectonic

This hypothesis often held for the Taiwanese orogen. Chapple (1978) defines thin-skinned fold-and-thrust belts parameters and considers that the global mechanics of these accretionary wedges is similar to those of the prisms which form in front of bulldozers. This theory has been tested by Davis et al. (1983) and Dahlen et al. (1984).

Davis et al. (1983) develop an analytic theory, which predicts the critical deformation of the prism materials in a compressive context. They quantitatively test this theory for the Taiwanese accretionary prism and obtain results in agreement with field observations. They suggest that the detachment is at the basal part of the Neogene continental margin, Dahlen et al. (1984) more precisely identified it in the Miocene and Pliocene layers. To define the thin-skinned cross-section (Fig. 2), we use a model inspired from the cross-section drawn by Malavieille and Trullenque (2009).

2.2. Thick-skinned tectonic

Some authors, using seismological data from Taiwan front orogen (Wu et al., 1997) or well-log and seismic reflection data (Hung et al., 1999) disagree with the thin-skinned tectonic. They propose that the detachment is actually in the basement. In this case, the

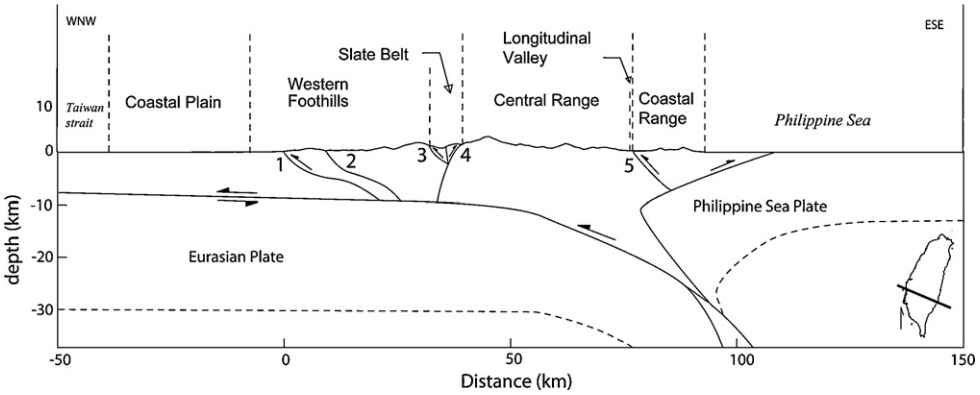

Fig. 2. Thin-skinned tectonic structure (after Malavieille and Trullenque, 2009). The detachment starts West at 10 km depth, between the basement and the sediment cover, and slopes down eastward below the Central Range. Faults join the detachment but do not cross it. Numbers refer to faults: 1—Lunhou, 2—Tingpinglin, 3—Tulungwan, 4—Lishan, 5—Longitudinal Valley fault.

deformation would be accommodated by the re-activation of normal faults created by the Paleogene rifting opening the Chinese Sea (Mouthereau and Petit, 2003), into reverse faults. According to Wu et al. (1997), the Taiwanese orogeny involves the whole crust and the upper mantle, in particular beneath the Central Range. They suggest lithospheric collision between the Eurasian and the Philippine Sea plates.

Mouthereau and Petit (2003) explain that, to accommodate this thick-skinned deformation, the detachment must belong to a weak part of the crust, probably at the brittle/ductile discontinuity. The dense fractures concentration in the upper crust compared to the lower crust and the lithospheric mantle make the latter appears less elastic and strong. The decoupling would then exists between the upper crust and the lower crust/mantle group. These indications are used to draw the thick-skinned structure (Fig. 3).

3. Deformation modeling

3.1. Elastic deformation modeling

Our elastic deformation code uses dislocation equations from Okada (1985, 1992) to compute the ground movements, vertically and horizontally, generated by faults slipping in an elastic half-space. The faults are defined by their geometry and their movement. After running, we compare the modeled horizontal movements with those measured by GPS. We proceed by trial and error to find the best adjustment between model and data. Attention is given to actual geophysics and geologic data already available from Taiwan structure to ensure the likelihood of our model.

We used the horizontal GPS velocities published by Hickman et al. (2002) based on measurements performed in 1996 and 1997. GPS velocities are computed relative to the SR01 station on Penghu Islands, i.e. in a Eurasia fixed reference frame. Due to the small interval between the measurements, vertical velocities are not usable to constrain the elastic models. Only GPS stations within a band of 10 km wide on both side of the studied transect are taken into account. Modeling will be performed using thick-skinned and thin-skinned models, for which geometries are different. However some basic modeling ideas are the same in both cases:

1. Faults are mapped following the geological map of Taiwan. We also add a large detachment beneath Taiwan. All the faults have a reverse movement.
2. The slip rate on the eastern part of the detachment is set to 82 mm yr^{-1}, corresponding to the Philippine Sea plate - Eurasian plate convergence rate (Yu et al., 1997).
3. The slip rate of the detachment decreases from East to West.
4. The faults start from the surface and stop on the detachment. They are divided into two segments to better represent their actual geometry, which dip is not constant (Hsu et al., 2003) and to allow depth-variable slip rates.
5. All the fault slip in depth and are locked close to the surface (Loevencruck et al., 2001) except the Longitudinal Valley fault where 30 mm yr^{-1} creep exists up to the surface (Lee et al., 2006).

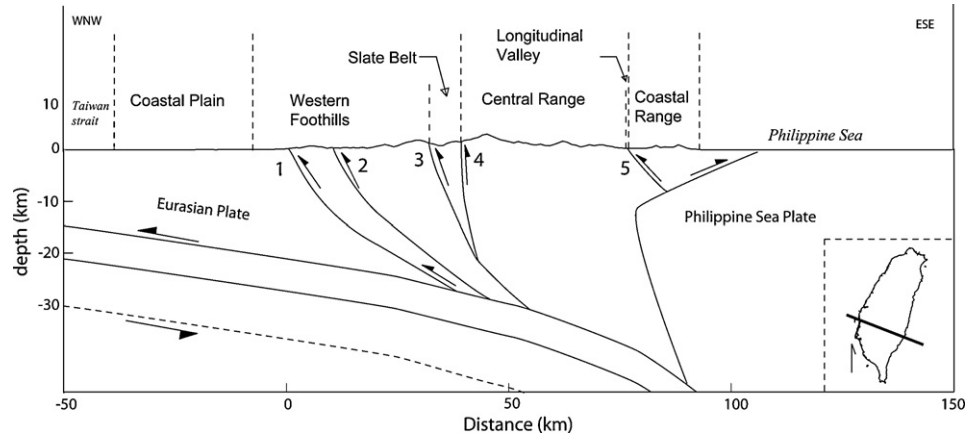

Fig. 3. Thick-skinned tectonic structure (after Mouthereau and Petit (2003) for the part West of the Central range). The detachment is deeper than in the thin-skinned structure, between the upper crust and the mantle. Also see Fig. 2 for faults numbers meaning.

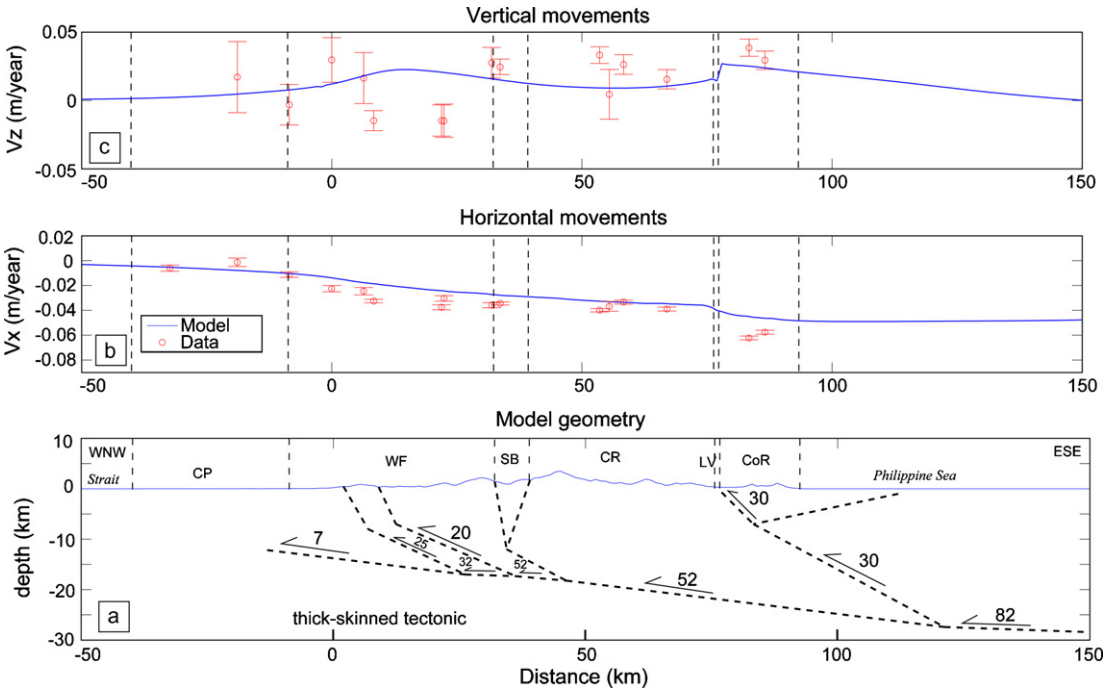

Fig. 4. From bottom to top: (a) model geometry and cinematic, faults are dashed lines, arrows indicates movements directions, values are slip velocities in mm yr^{-1}. Abbreviations: CP = Coastal Plain; WF = Western Foothills; SB = Slate Belt; CR = Central Range; LV = Longitudinal Valley; CoR = Coastal Range. (b) Horizontal movements measured (red circles) and modeled (plain blue line), positive values mean eastward movement. (c) Vertical movements measured (red circles) and modeled (plain blue line), positive values mean upward movement. We adjust modeled horizontal movements to estimated ones. (For interpretation of the references to color in this figure legend, the reader is referred to the web version of the article.)

6. Apart the Longitudinal Valley, the shortening of Taiwan is mostly accommodated within the Western Foothills faults (Simoes and Avouac, 2006). We consequently assume higher slip rate in this region.

3.2. Thick-skinned tectonic results

The best-fit model is shown on Fig. 4. The detachment starts from the West at 15 km depth and slightly dips (3°) to the East (Fig. 4a). This model underestimates the westward velocities in the Western Foothills and the Coastal Range, respectively 20% and 17% lower (Fig. 4b). These too low velocities are due to the highly dipping faults, which cannot generate strong horizontal movements but return high vertical movements (Fig. 4c). Moreover, due to the depth of the detachment, the faults slip at great depth, reducing the movement created on the ground.

The thick-skinned model returns vertical movements from 0 to 2.6 cm yr^{-1}, i.e. only surrection. The greatest elevation rates are in the Western Foothills and in the Coastal Range, where there are reverse faults. It illustrates the upward movement of their hanging wall. The Longitudinal Valley fault returns the higher elevation rate, 2.6 cm yr^{-1}, in the Coastal Range.

3.3. Thin-skinned tectonic results

Here the detachment starts at 5 km depth, beneath the Coastal Plain and slopes down to 10 km depth beneath the Coastal Range, with 3° dip (Fig. 5a). This model fits well the horizontal GPS velocities (Fig. 5b). This agrees with Hsu et al. (2003) who have shown that a thin-skinned model is able to fit the horizontal GPS velocities.

Vertical movements (Fig. 5c) remain higher in the Western Foothills and the Coastal Plain, but are not as great and wide as with the thick-skinned model. We predict 1.5 cm yr^{-1} of maximum elevation versus 2.6 cm yr^{-1} with the thick-skinned tectonic. Thin-skinned tectonic involves faults with a lower dip, which slip creates high horizontal movements but small vertical movements. This is well illustrated by comparing movements generated by the Longitudinal Valley, Tingpinglin or Lunhou faults for each model (Figs. 4 and 5). Consequently westward movements are not underestimated anymore and the modeled elevation rate decreases in the Western Foothills. The other parameter improving the adjustment of the model to the horizontal GPS velocities is the lower depth of the detachment, its slip is less attenuated on the ground since it is closer to the surface than it was with the thick-skinned tectonic. No particular surrection of the Central Range is predicted, even with the thick-skinned model. This is characteristic of any model in which most of the convergence is transferred across Taiwan to the Western Foothills (Hsu et al., 2003).

4. Gravity modeling

We use Granom (Hetényi et al., 2007), a code computing gravity anomaly based on Won and Bevis (1987) algorithm, to calculate the gravity changes involved by the deformation modeled in Section 3. Applying densities on the 2D structure, we calculate the gravity anomaly generated before and after the elastic deformation. Subtracting these anomalies from each other, the gravity change owing to deformation is obtained.

4.1. Density model

In addition to an increase of the density value with depth, the strong lateral heterogeneity of materials in Taiwan is also taken into account. Sediments in the Coastal Plain are little condensed while the orogen, which extends from the Western Foothills to the Coastal Range, experiences exhumation of deep, i.e. high density, rocks (Dahlen et al., 1984). The Coastal Range, as part of the oceanic crust, is denser than continental crust materials. According to Dahlen et al. (1984) and Lin and Watts (2002), the following scheme is applied:

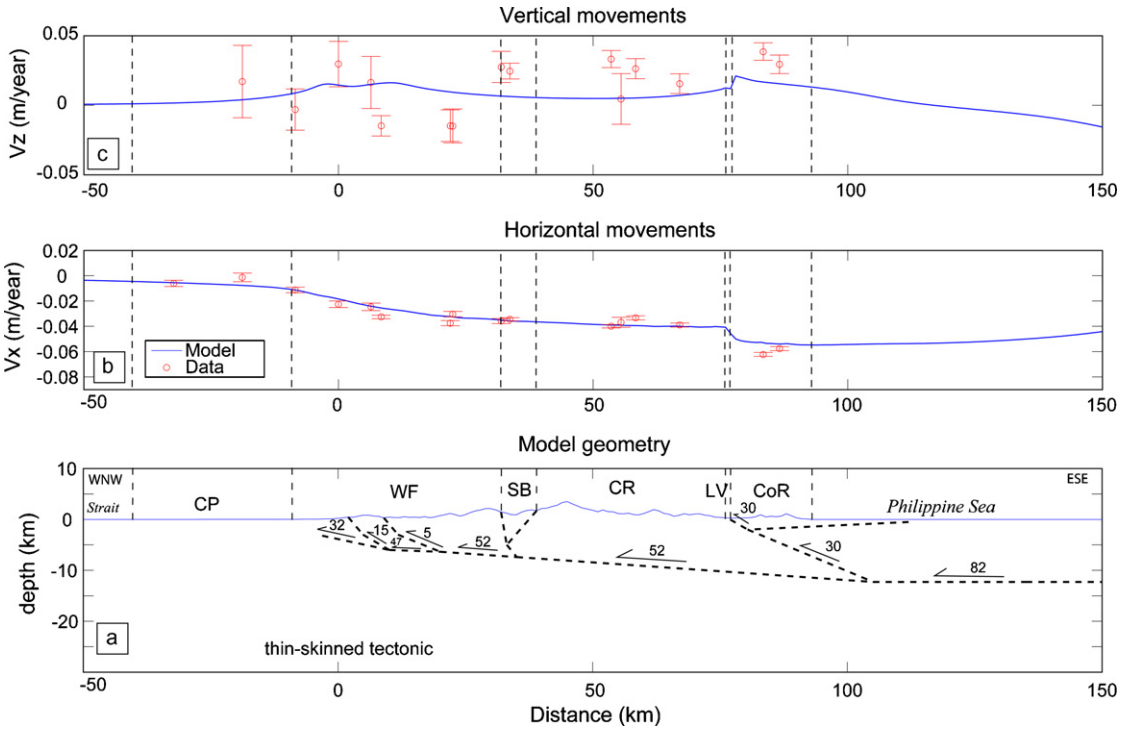

Fig. 5. Same as Fig. 4 but considering a thin-skinned tectonic. This geometry allows a better adjustment of modeled horizontal movements to estimated ones, in particular in the Western Foothills and the Longitudinal Valley. Also see Fig. 4 for abbreviations.

1. Sedimentary basin (Coastal Plain): 2.5 (2500 kg m^{-3}).
2. Topographic load (Western Foothills, Slate Belt and Central Range) and middle crust: 2.7 (2700 kg m^{-3}).
3. Oceanic crust (Coastal Range and eastern regions) and lower crust: 2.8 (2800 kg m^{-3}).

Areas of different densities are bounded with the faults and depth threshold used in each model. Hence the regions with same density will have different size depending on the tectonic model, thick or thin-skinned.

4.2. Modeling

Whatever the tectonic, comparing the elevation rate modeled (Fig. 6a and b) with gravity changes (Fig. 6c) underlines the free-air effect, the gravity decreases when altitude increases. The shape of gravity changes is indeed the opposite to vertical movements. Using the mean free-air gradient −0.3086 mGal for one meter elevation, we remove this effect and obtain the Fig. 6d.

The plate effect is here well illustrated as gravity changes have the same trend as vertical elevation. This can be demonstrated plotting gravity changes versus elevation rate, which gives a slop of 0.1138 mGal m^{-1} with a good determination coefficient. If we now estimate the plate effect using the mean 0.0419 ρ mGal m^{-1} and a mean density 2.67, we obtain 0.1118 mGal m^{-1}, which is very close to the slope given in regression equation. Gravity changes are then dominated by free-air and plate effect, involving several Gal of change each year.

Also removing plate effect we obtain gravity changes only due to mass transfers (Fig. 7). They are low, around ten times smaller than free-air and plate effects. The thick-skinned tectonic returns higher gravity changes, up to 0.3 Gal yr^{-1} while the thin-skinned tectonic profile is almost constant, near zero. The step at distances 0 and 80 km, for both tectonics, may be explained by the lateral change of density at the surface, respectively from 2500 to 2700 kg m and 2700 to 2800 kg m^{-3} and do not give indications on deep mass transfers. The thick-skinned signal in the east part of Taiwan may be interpreted as the overhang of the Coastal Range and oceanic crust dense rocks on the continental crust beneath the Central Range. The gravity decrease, which extends from the Western Foothills to the Central Range, is more complicated to explain. One hypothesis could be the slip on the detachment and the global westward propagation of the whole system, which slightly replaces lower crust with upper material, less dense.

With more confidence we can suggest that the thick-skinned tectonic generates higher gravity changes since, with its geometry, it involves higher rock volumes, hence higher mass transfers.

5. Discussion

We obtain the best fit between the modeled horizontal velocities and those estimated by GPS using the thin-skinned tectonic geometry. The thick-skinned tectonic can model the global trend of the westward horizontal movements, i.e. a growing amplitude from West to East, but quantitatively values are underestimated of ∼20%. Yet we do not reject this tectonic hypothesis since the horizontal GPS velocities we used contain uncertainties involved by the short delay between campaigns (see Section 3.1). Hence, they cannot be considered as absolute discriminant factors. In addition we use elastic modeling, which may show limitations when applied for complex rheology. The fact that we do not represent the subduction of the Eurasian plate beneath the Philippine Sea plate betrays this limitation: it exists in the region we study, consequently the detachment we draw beneath Taiwan should slop down eastward with an increasing dip. But this geometry fails to make modeled horizontal velocities fit GPS data.

Concerning vertical movements, Chen (1984) found that the Central Range rises faster than the Coastal Range but we do not retrieve this observation. West of the Longitudinal Valley the modeled shortening is accommodated by faults of the Western Foothills, which consequently rises. Our elastic model cannot generate surrection in the Central range since there is no active fault in this

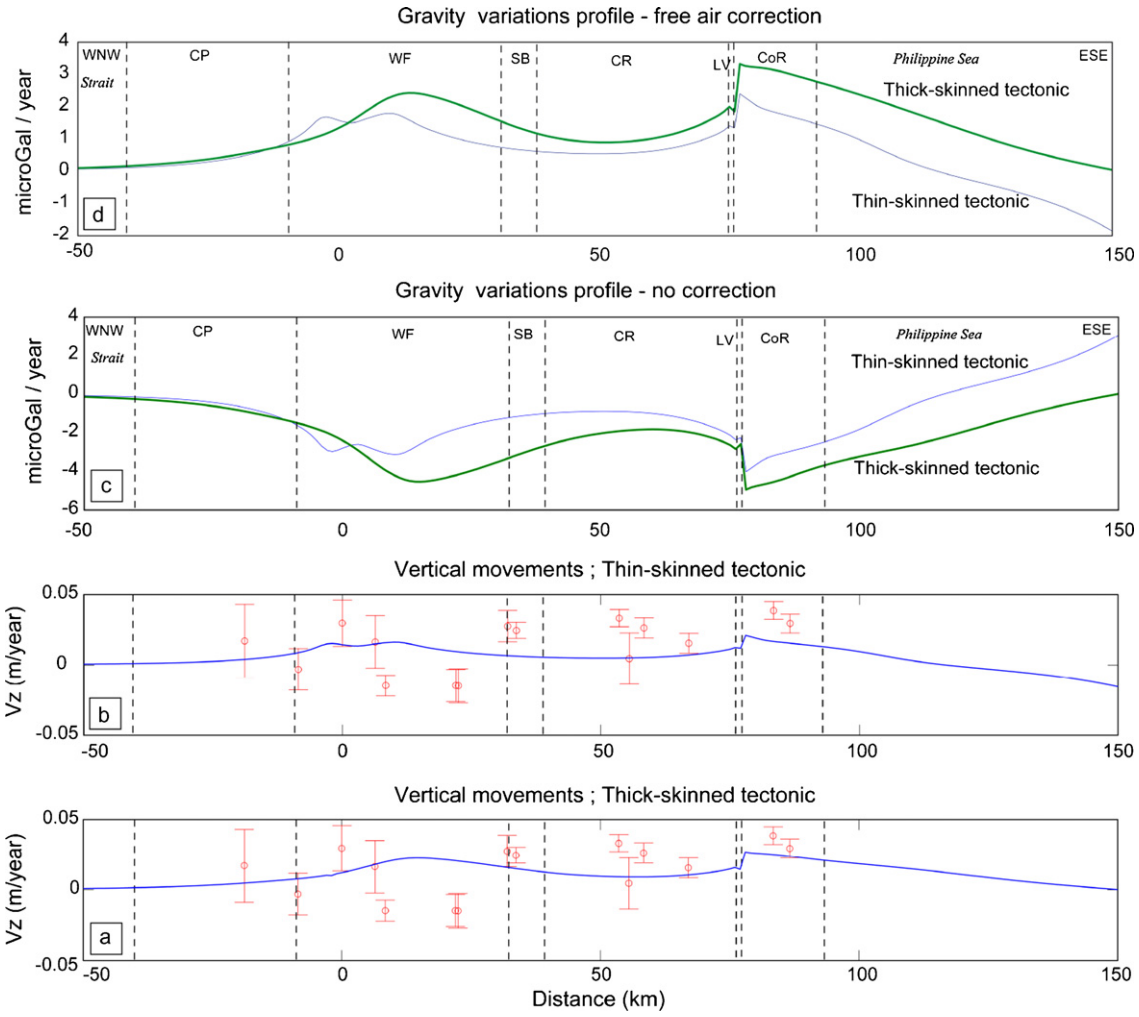

Fig. 6. Graphs (a) and (b) are respectively the modeled vertical movements for thick-skinned tectonic and thin-skinned tectonic (already shown in Figs. 4 and 5c). (c) Gravity changes modeled with thin (fine blue line) and thick-skinned (bold green line) tectonic. Note the symmetry between vertical movements and the gravity signal, which reflects free-air effect. (d) Same as (c) but the gravity signal has been corrected from free-air effect. Its shape has now the same trend as vertical movements, for each tectonic. The plate effect is here responsible for the main part of the gravity signal. Also see Fig. 4 for abbreviations. (For interpretation of the references to color in this figure legend, the reader is referred to the web version of the article.)

region. Simoes and Avouac (2006) suggest that the Central Range surrection can be explained by underplating of the upper seven km of the Eurasian crust beneath the orogen, during the convergence of the Philippine Sea plate toward the Chinese continental margin. The shortening accommodation occurs in the Western Foothills where an accretionary prism grows, but there is no accretion in the intern part of the orogen; its rising and exhumation are consequences of this underplating. It is typically a deep mass transfer and must be taken into account for accurate gravity modeling. Behavior finer than pure elasticity, allowing thermokinematic deformation, is likely to simulate this phenomenon.

The vertical movements of the Central Range lead to two major issues. The first one is the uncertainty attributed to GPS data; determining vertical velocities using GPS requires at last one decade to obtain robust results. The second one is to use the appropriate deformation model to fit the vertical velocities. Both issues involve uncertainty of the estimation of the gravity signal due to vertical movement, i.e. free-air and plate effect, which represent the most important part of the total gravity signal expected from mountain building. The mass transfer gravity signal, far smaller in comparison, has consequently a large uncertainty.

One must note that we do not model any hydrological effect. Yet it can reaches values above 10 μGal due to local variations of groundwater height (Naujoks et al., 2008; Jacob et al., 2008). This amplitude may hide or deprave the expected tectonic effects; some μGal per year according to our modeling. Actually, AG sites have been also selected to minimize hydrological influence. From AG1 to AG6, pillars are located in mountains and directly built on the rock basement. Water is supposed to bypass in these areas without being stored inside the thin soil cover. Nevertheless, this situation is not possible for AG7 and AG8, which are in the Coastal Plain, i.e. a sedimentary basin covering the west side of Taiwan and containing several aquifers. We must hence pay special attention to groundwater height for these two sites, using aquifer monitoring performed in Taiwan. Moreover aquifers in this region suffer from over-pumping involving subsidence rates higher than 1 cm yr^{-1} (Hou et al., 2005; Hu et al., 2006). This movement is likely to have effect on gravity value but must absolutely be identified since we just consider tectonic phenomena.

Modern absolute gravimeters have a sensitivity around 1 μGal, yet the gravity changes we model, only concerning mass transfers, reaches maximum 0.3 μGal yr^{-1}. At least three years are hence needed between two measurements to see deep mass transfer effects. But only one year should offers interesting results since we predict up to 5 μGal yr^{-1} due to elevation. AGTO should consequently sort out the tectonic component of gravity in Taiwan.

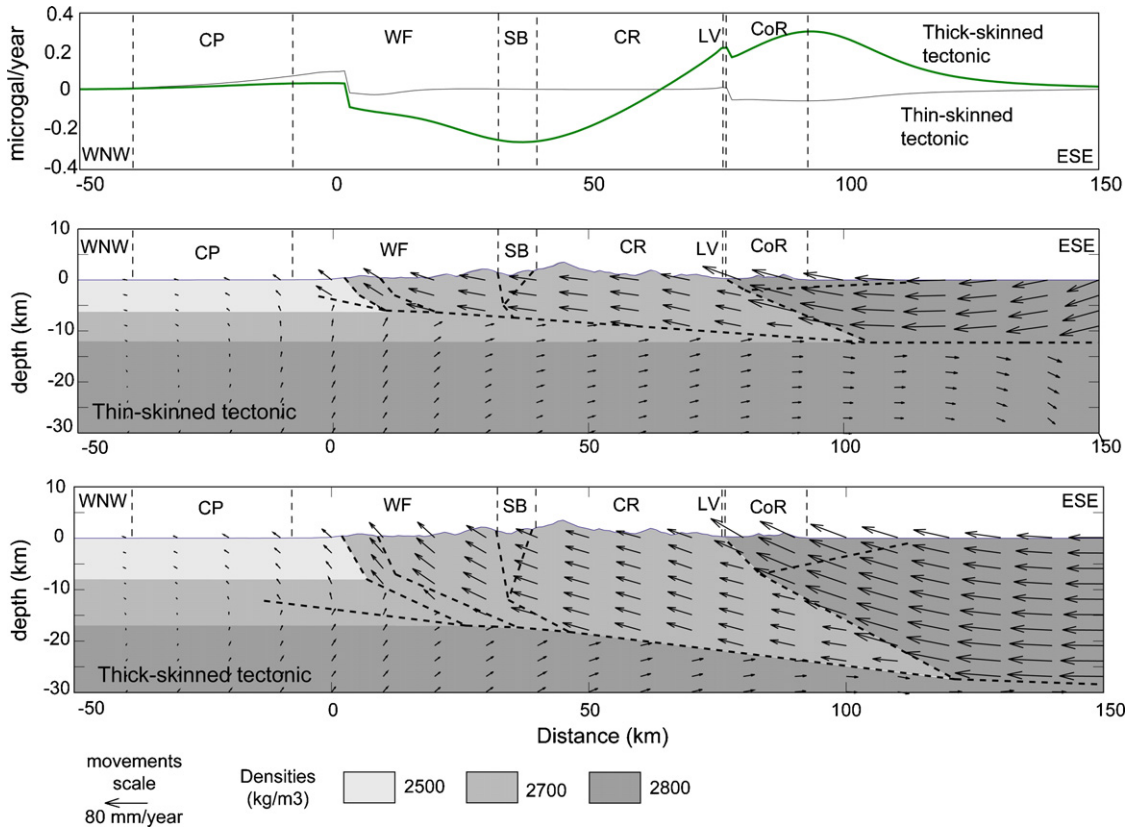

Fig. 7. Gravity changes modeled for the two hypothesis, thin-skinned (fine blue line) and thick-skinned tectonic (bold green line), and only due to mass transfers. Free-air and plate effects have been removed. The thick-skinned tectonic returns the higher gravity changes in the Coastal range with 0.3 μGal yr^{-1}, while the thin-skinned tectonic reaches maximum 0.1 μGal yr^{-1}. The greyscale gives the density model and the arrows indicate the structure movements. Also see Fig. 4 for abbreviations. (For interpretation of the references to color in this figure legend, the reader is referred to the web version of the article.)

6. Conclusion

The aim of this paper was to give preliminary ideas of what signal can be expected from the AGTO project, using elastic deformation and gravity modeling for two main tectonic contexts: thick-skinned and thin-skinned. Our results show higher elevation rates in the Western Foothills and the Coastal Range reaching respectively 1.5 and 2 cm yr^{-1} for the thin-skinned tectonic and 2.2 and 2.6 cm yr^{-1} for the thick-skinned. The gravity changes are maximum in the same regions; respectively 3.8 and 4 μGal yr^{-1} for the thin-skinned tectonic and 4.5 and 5 Gal yr^{-1} for the thick-skinned. Yet most of this signal is free-air and plate effects, mass transfers effects are ten times lower: 0.1 μGal yr^{-1} assuming a thin-skinned tectonic and 0.3 μGal yr^{-1} with the thick-skinned. Both are expected in the Coastal Range where density contrast and movement along the Longitudinal Valley, the plate boundary between Eurasian and the Philippine Sea plates, are significant. As this yearly signal is very low, it will be difficult to identify without robust GPS and hydrological constraints and long time series. Our modeling fails to reproduce the Central Range surrection, which is known to be the fastest elevated region of Taiwan (Chen, 1984; Hsu et al., 2003; Wu et al., 1997). Such a misfit can be related to the elastic behavior we assume in our modeling, while a more complicated rheology may be involved. This surrection is supposed to be driven by underplating below the orogen (Simoes and Avouac, 2006), that we do not model in our study. The absolute gravity measurements will first reflect the vertical movements in Taiwan and then deep mass transfers for which several years of measurement should be needed before any interpretation. GPS measurements will have a strong interest to precisely separate elevation and deep mass transfer effects.

Acknowledgments

We are grateful to John B. Hickman for providing us with GPS velocities data. We also thank György Hetényi for his guidance in our use of Granom program. Fig. 1 has been drawn with Generic Mapping Tools – GMT (Wessel and Smith, 1998).

References

Angelier, J., 1986. Preface. Tectonophysics, 125.
Chapple, W.M., 1978. Mechanics of thin-skinned fold-and-thrust belts. Geol. Soc. Am. Bull. 89, 1189–1198.
Chen, H., 1984. Crustal uplift and subsidence in Taiwan: an account based upon retriangulation results. Spec. Publ. Cent. Geol. Surv. 3, 127–140.
Dahlen, F.A., Suppe, J., Davis, D., 1984. Mechanics of fold-and-thrust belts and accretionary wedges: cohesive Coulomb theory. J. Geophys. Res. 89 (B12), 10,087–10,110.
Davis, D., Suppe, J., Dahlen, F.A., 1983. Mechanics of fold-and-thrust belts and accretionary wedges. J. Geophys. Res. 88 (B2), 1153–1172.
Hetényi, G., Cattin, R., Brunet, F., Bollinger, L., Vergne, J., Nábelek, J.L., Diament, M., 2007. Density distribution of the India plate beneath the Tibetan Plateau: geophysical and petrological constraints on the kinetics of lower-crustal eclogitization. Earth Planet. Sci. Lett. 264 (1–2), 226–244, doi:10.1016/j.epsl.2007.09.036.
Hickman, J.B., Wiltschko, D.V., Hung, J.-H., Fang, P., Bock, Y., 2002. Structure and evolution of the active fold-and-thrust belt of southwestern Taiwan from Global Positioning System analysis. In: Byrne, T.B., Liu, C.-S. (Eds.), Geology and Geophysics of An Arc-Continent Collision, Taiwan. Geological Society of America Special Paper, Boulder, CO # 358, pp. 75–92.
Ho, C.S., 1986. A synthesis of the geologic evolution of Taiwan. Tectonophysics 125, 1–16.
Hou, C.-S., Hu, J.-C., Shen, L.-C., Wang, J.-S., Chen, C.-L., Lai, T.-C., Huang, C., Yang, Y.-R., Chen, R.-F., Chen, Y.-G., Angelier, J., 2005. Estimation of subsidence using GPS measurements, and related hazard: the Pingtung Plain, southwestern Taiwan. C. R. Geosci. 337, 1184–1193.
Hsu, Y.-J., Simons, M., Yu, S.-B., Kuo, L.-C., Chen, H.-Y., 2003. A two-dimensional dislocation model for interseismic deformation of the Taiwan mountain belt. Earth Planet. Sci. Lett. 211, 287–294.

Hu, J.-C., Chu, H.-T., Hou, C.-S., Lai, T.-H., Chen, R.-F., Nien, P.-F., 2006. The contributor to tectonic subsidence by groundwater abstraction in the Pingtung area, southwestern Taiwan as determined by GPS measurements. Quat. Int. 147, 62–69.

Hung, J.-H., Wiltschko, D.V., Lin, H.-C., Hickman, J.B., Fang, P., Bock, Y., 1999. Structure and motion of the southwestern Taiwan fold-and-thrust belt. TAO 10 (3), 543–568.

Jacob, T., Bayer, R., Chéry, J., Jourde, H., Le Moigne, N., Boy, J.-P., Hinderer, J., Luck, B., Brunet, P., 2008. Absolute gravity monitoring of water storage variation in a karst aquifer on the larzac plateau (Southern France). J. Hydrol. 359, 105–117.

Karner, G.D., Watts, A.B., 1983. Gravity anomalies and flexure of the lithosphere at mountain ranges. J. Geophys. Res. 88 (B12), 10,449–10,477.

Lee, J.-C., Chu, H.-T., Angelier, J., Hu, J.-C., Chen, H.-Y., Yu, S.-B., 2006. Quantitative analysis of surface coseismic faulting and postseismic creep accompanying the 2003, Mw = 6.5, Chengkung earthquake in eastern Taiwan. J. Geophys. Res. 111, B02405, doi:10.1029/2005JB003612.

Lin, A.T., Watts, A.B., 2002. Origin of the west Tainan basin by orogenic loading flexure of a rifted continental margin. J. Geophys. Res. 107 (B9), 2185, doi:10.1029/2001JB000669.

Loevencruck, A., Cattin, R., Le Pichon, X., Courty, M.-L., Yu, S.-B., 2001. Seismic cycle in Taiwan derived from GPS measurments. C. R. Acad. Sci. Paris, Earth. Planet. Sci. Lett. 333, 57–64.

Malavieille, J., Trullenque, G., 2009. Consequences of continental subduction on forearc basin and accretionary wedge deformation in SE Taiwan: insights from analogue modeling. Tectonophysics 466, 377–394.

Mouthereau, F., Petit, C., 2003. Rheology and strength of the Eurasian continental lithosphere in the foreland of the Taiwan collision belt: constraints from seismicity, flexure, and structural styles. J. Geophys. Res. 108 (B11), 2512, doi:10.1029/2002JB002098.

Naujoks, M., Weise, A., Kroner, C., Jahr, T., 2008. Detection of small hydrological variations in gravity by repeated observations with relative gravimeters. J. Geod. 82, 543–553, doi:10.1007/s00190-007-0202-9.

Okada, Y., 1985. Surface deformation due to shear and tensile faults in a half-space. Bull. Seism. Soc. Am. 75, 1135–1154.

Okada, Y., 1992. Internal deformation due to shear and tensile faults in a half-space. Bull. Seism. Soc. Am. 82, 1018–1040.

Simoes, M., Avouac, J.P., 2006. Investigating the kinematics of the mountain building in Taiwan from the spatiotemporal evolution of the foreland basin and western foothills. J. Geophys. Res. 111, B10401, doi:10.1029/2005JB004209.

Segall, P., Davis, J.L., 1997. GPS applications for geodynamics and earthquake studies. Annu. Rev. Earth Planet. Sci. 25, 301–336.

Suppe, J., 1980. A retrodeformable cross section of northern Taiwan. Geol. Soc. China Proc. 23, 46–55.

Torge, W., 1990. Absolute gravimetry as an operational tool for geodynamics research. In: Developments in Four-Dimensional Geodesy. Book Series Lecture Notes in Earth Sciences, vol. 29. Springer, Berlin /Heidelberg, pp. 15–28.

Wessel, P., Smith, W.H.F., 1998. New, improved version of generic mapping tools released. EOS Trans. Am. Geophys. U. 79 (47), 579.

Won, I.J., Bevis, M., 1987. Computing the gravitational and magnetic anomalies due to a polygon: algorithms and Fortran subroutines. Geophysics 52, 232–238.

Wu, F.-T., Rau, R.-J., Salzberg, D., 1997. Taiwan orogeny: thin-skinned or lithospheric collision? Tectonophysics 274, 191–220.

Yu, S.-B, Chen, H.-Y., Kuo, L.-C., 1997. Velocity field of GPS stations in the Taiwan area. Tectonophysics 274, 41–59.